J. Eng. Technol. Sci., Vol. 53, No. 4, 2021, 210402

Theoretical Study of Direct Carbon Dioxide Conversion to Formic Acid on Transition Metal-doped Subnanometer Palladium Clusters

Adhitya Gandaryus Saputro[1,2,*], Arifin Luthfi Maulana[1], Fine Dwinita Aprilyanti[1] & Hermawan Kresno Dipojono[1,2]

[1]Advanced Functional Materials Research Group, Faculty of Industrial Technology, Institut Teknologi Bandung, Jalan Ganesha 10, Bandung 40132, Indonesia
[2]Research Center for Nanosciences and Nanotechnology, Institut Teknologi Bandung, Jalan Ganesha 10, Bandung 40132, Indonesia
*E-mail: ganda@tf.itb.ac.id

Highlights:

- Transition metal-doped subnanometer palladium clusters were used as catalyst for direct CO_2 hydrogenation to formic acid without the presence of base additives.
- The transition metal-doped subnanometer palladium clusters were more selective toward CO_2 hydrogenation to formic acid than the reverse water gas shift reaction.
- The nickel doped palladium cluster system had the best turnover frequency for formic acid formation.

Abstract. We studied the direct conversion of CO_2 to HCOOH through hydrogenation reaction without the presence of base additives on the transition metal-doped subnanometer palladium (Pd_7) cluster (Pd_xM: M = Cu, Ni, Rh) by using a combination of density functional theory and microkinetic calculations. It was shown that the CO_2 hydrogenation on Pd_7 and Pd_6M clusters are more selective towards the formate pathway to produce HCOOH than the reverse water gas shift pathway to produce CO. Inclusion of Ni and Rh doping in the subnanometer Pd_7 cluster could successfully enhance the turnover frequency (TOF) for CO_2 hydrogenation to formic acid at low temperature. The order of TOF for formic acid formation is as follows: $Pd_6Ni > Pd_6Rh > Pd_7 > Pd_6Cu$. This order can be explained by the trend of the activation energy of CO_2 hydrogenation to formate ($HCOO^*$). The Pd_6Ni cluster has the highest TOF value because it has the lowest activation energy for the formate formation reaction. The Pd_6Ni system also has a superior TOF profile for HCOOH formation compared to several metal surfaces in low and high-temperature regions. This finding suggests that the subnanometer Pd_xNi cluster is a promising catalyst candidate for direct CO_2 hydrogenation to formic acid.

Keywords: *CO_2 hydrogenation; density functional theory; formic acid; microkinetic; subnanometer Pd cluster; transition metal doping.*

Received May 19th, 2020, 1st Revision October 29th, 2020, 2nd Revision February 28, 2021, Accepted for publication April 12th, 2021.
 ISSN: 2337-5779,
DOI: 10.5614/j.eng.technol.sci.2021.53.4.2

1 Introduction

The conversion of carbon dioxide (CO_2) to valuable chemicals is one of humanity's grand schemes to battle the threat of global warming [1-4]. Among these schemes is the direct CO_2 conversion to formic acid (HCOOH) through a series of hydrogenation reactions [4]. This scheme is important owing to the potential applications of formic acid. It can be employed as chemical feed for producing more complex chemical structures, reversible hydrogen storage, and also as input for fuel cells to generate electricity [4].

The process of CO_2 hydrogenation to HCOOH on a heterogeneous catalyst system possesses many benefits as compared to a homogeneous catalyst, including simple product separation, good catalyst stability, easy handling, and easy usability [4,5]. Unfortunately, the catalytic activity of heterogeneous catalysts for this process is currently still limited. Some of the factors causing the low catalytic activity are the endergonic profile of the conversion process, the inertness of the CO_2 molecules, and the existence of high activation energies for the hydrogenation reactions. To improve the catalytic activity, the presence of additional base solutions is required to make the reaction exergonic [4,5].

In recent years, supported palladium-based nanoparticles on metal-oxide and carbon-based materials have been reported to give excellent catalytic activities toward CO_2 hydrogenation to HCOOH in the presence of base additives [4,6-11]. While the presence of bases is important, the possibility of omitting them is quite intriguing since it allows for the elimination of the additional product purification step and the product can also be separated with simple filtration [12]. The work of Nguyen *et al.* was the first to experimentally show that CO_2 hydrogenation to HCOOH in the absence of base additives can actually be realized at relatively low pressure by using supported Pd-Ni alloy nanoparticles on CNT-graphene composite, even though the catalytic activity is still relatively low [12]. More efforts are needed to enhance the ability of Pd-based nanoparticles to directly convert CO_2 to HCOOH without the presence of base additives. This enhancement may be achieved if we can find a catalyst that can easily activate CO_2 molecules and improve the reaction profiles for the elementary hydrogenation reactions.

In our previous study [13], we compared the ability of a small subnanometer Pd cluster (Pd_x) and supported large-Pd nanoparticles on metal oxide to catalyze the CO_2 hydrogenation to methanol. We found that a large-Pd island can only act as an H_2 dissociation center when the oxide surface acts as the CO_2 hydrogenation center. On the other hand, the Pd_x clusters can act not only as an H_2 dissociation center but also as a CO_2 hydrogenation center. One of the reasons is that the Pd_x clusters can easily activate inert CO_2 molecules by donating some charges to the

anti-bonding orbital of the CO_2 molecules, which enhances the repulsion inside the molecules. To minimize this repulsion, the CO_2 molecules break their linear O-C-O angle, which results in a bidentate adsorption configuration. The bidentate adsorption configuration weakens the C-O bonds inside the adsorbed CO_2 molecules and makes the molecules more reactive. All of these features indicate that a small subnanometer Pd_x cluster may be used as the foundation for designing a new catalyst for direct CO_2 hydrogenation to HCOOH.

As an attempt to overcome the challenge of excluding base additives, in this study we tried to use small (subnanometer) Pd_x clusters doped by transition metals (Pd_xM; M = Cu, Ni, and Rh) as catalyst candidate for CO_2 hydrogenation to HCOOH. We previously found that the addition of these transition metal dopings to a subnanometer Pd_7 cluster can intensify its interaction with the CO_2 molecules and also allows the molecules to be bent and adsorbed with a bidentate adsorption configuration [14]. This strong interaction may have a positive effect on the ability of the cluster to catalyze the CO_2 hydrogenation to HCOOH.

We performed systematic density functional theory (DFT) calculations to simulate the elementary reactions of CO_2 hydrogenation to HCOOH on the Pd_xM clusters. The calculated adsorption energies, reaction energies, and activation energies of the elementary reactions from the DFT calculations were utilized to perform microkinetic simulations to obtain the turn-over frequencies (TOFs) of the CO_2 hydrogenation reaction on the Pd_xM clusters as a measure of their reactivity.

2 Computational Details

2.1 Cluster Models

We chose the Pd_7 cluster structure from our previous study as the basic model to represent small subnanometer Pd_x clusters [13]. The size of this cluster is large enough to accommodate the co-adsorption of CO_2 hydrogenation-related reactants and products. This cluster model has also been successfully used to study the HCOOH decomposition reaction [15]. In a more realistic catalyst model, the subnanometer Pd_x cluster should be placed on a support material. However, our previous study showed that the Pd_7 cluster maintained its original structure when it was deposited on a metal oxide surface, even though insignificant geometrical reconstructions were induced by the corrugated nature of the metal oxide surface [13]. Moreover, we also showed that the adsorption properties of the CO_2 molecules on this cluster did not change in the presence of a support material. Therefore, for the sake of simplicity, here we used an unsupported subnanometer Pd_7 cluster for modeling the CO_2 hydrogenation reactions.

We constructed a transition metal doped Pd_7 model by substituting one of the Pd atoms in the cluster with a transition metal atom M (Pd_6M). We then compared the total energies for all of the seven possible substitution sites. The configuration that gave the lowest total energy was chosen as the model for the Pd6M cluster. This procedure was repeated for all of the M atoms (M = Cu, Ni, and Rh). The most stable structure of the Pd_7 and Pd_6M clusters were taken from reference [14], as presented in Figure 1.

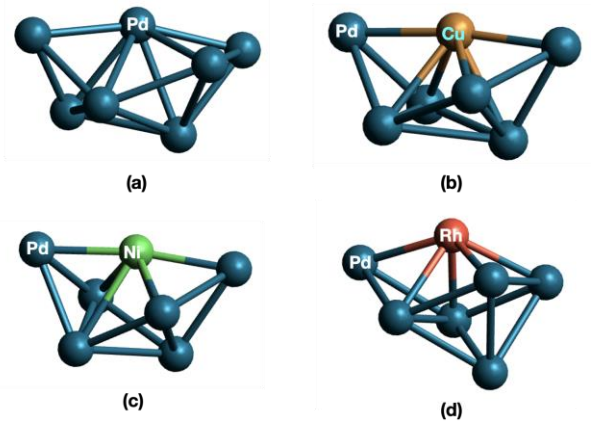

Figure 1 The most stable structures of (a) Pd_7, (b) Pd_6Cu, (c) Pd_6Ni, and (d) Pd_6Rh clusters.

2.2 DFT Calculations and Microkinetic Modeling

We utilized density functional theory (DFT) calculations to study the CO_2 hydrogenation to HCOOH on the Pd_7 and Pd_6M clusters. The DFT calculations were performed using the Gaussian09 software package. We used the same calculation parameters as in our previous study about CO_2 conversion to methanol on small Pd_x clusters. The B3LYP functional was used as the exchange-correlation potential. We used the 6-311++G^{**} basis sets for light atoms (H, C, and O), and the LANL2DZ basis sets with effective core potentials for the transition metal atoms (Pd, Cu, Ni, and Rh).

The adsorption energy (E_{ads}) of a molecule on a Pd_6M cluster was calculated using Eq. (1):

$$E_{ads} = E_{system} - (E_{Pd6M} + E_{mol}) + \Delta ZPE, \quad (1)$$

where E_{system} corresponds to the total energy of the adsorption system, E_{Pd6M} corresponds to the total energy of the isolated Pd_6M cluster, and E_{mol} corresponds to the total energy of the isolated molecule. ΔZPE corresponds to the difference in the zero-point energy correction for the total system and the isolated systems.

The corresponding spin configurations for the calculation of E_{system}, E_{Pd6M} and E_{mol} are set in their respective spin ground state configurations.

The activation energy for an elementary reaction (E_{act}) was calculated using Eq. (2):

$$E_{act} = E_{ts} - E_{is}, \quad (2)$$

where E_{ts} and E_{is} correspond to the total energy of the initial state and the transition state of the elementary reaction. The structure and the energy of the transition state were calculated using the synchronous transit-guided quasi-newton (STQN) method. We affirm that the obtained transition state structure only has one imaginary frequency.

The obtained energetical data from the DFT calculations were used as inputs for microkinetic simulations to obtain the turnover frequencies (TOFs) of CO_2 hydrogenation reactions. We used Eqs. (3) and (4) to address the adsorption and desorption reactions:

$$k_{ads} = \frac{A}{\sqrt{2\pi m k_B T}} \exp\left(-\frac{E_{ads}}{k_B T}\right) \quad (3)$$

$$k_{des} = \frac{k_B T^3}{h^3} \frac{A(2\pi m k_B)}{\sigma \Theta_{rot}} \exp\left(-\frac{E_{des}}{k_B T}\right) \quad (4)$$

where A is the active site catalytic surface, m is the molecular mass of the gas, σ is the symmetry number of the molecule, and Θ_{rot} is the characteristic rotational temperature of the molecule. E_{ads} and E_{des} represent the adsorption and desorption energy, respectively. The rate for surface reactions was treated using Eq. (5):

$$k = \frac{k_B T}{h} \exp\left(-\frac{E_a}{k_B T}\right) \quad (5)$$

where E_a is the reaction activation energy. We ignored the partition function ratio due to negligible entropy change.

The overall rate of each elementary step can be written as the difference between the forward and backward reaction rates:

$$r_i = k_{f,i} \prod_{j \in IS} P_j \theta_j - k_{b,i} \prod_{j \in FS} P_j \theta_j \quad (6)$$

where r_i is the rate of elementary step i, P_j is the partial gas pressure of species j, and θ_j is the fractional coverage of species j. The rate of change of all coverages can be expressed using Eq. (7):

$$\frac{d\theta_j}{dt} = \sum_{i \in FS} n_i r_i - \sum_{i \in IS} n_i r_i \quad (7)$$

where n_i is the number of adsorbate j being produced (left term) or consumed (right term) in elementary step i. The sum of all coverages has to be conserved. This condition is expressed using Eq. (8):

$$\sum_j \theta_j = 1 \tag{8}$$

Details of the microkinetic model derivation for typical hydrogenation reaction can be found in our recent works [13,16-18].

To estimate the contribution of each step to the overall reaction rate, we used Campbell's degree of rate control (XRC) [19,20], which can be defined using Eq. (9):

$$XRC_i = \left(\frac{\partial \ln r}{\partial \ln k_i}\right)_{K_i, k_{i \neq j}} \tag{9}$$

where the calculation holds the equilibrium constant of step i (K_i) and the rate constant of step j (where $i \neq j$) to be unvarying.

3 Results and Discussions

3.1 HCOOH vs CO Formations

The initial CO_2 hydrogenation step (CO_2^* + H^*) may result in two different reaction pathways. The first possibility is the formation of an adsorbed formate ($HCOO^*$), which leads to the formation of HCOOH, the desired product of this study. This reaction pathway is known as the formate pathway. The second possibility is the formation of an adsorbed hydrocarboxyl ($HOCO^*$), which leads to the formation of carbon monoxide (CO) and water (H_2O) molecules. The second pathway is known as the reverse water gas shift reaction (RWGS). The energetical data for CO_2 hydrogenation through the formate and RWGS pathways is presented in Table 1.

The sequence of elementary reactions for the formation of HCOOH through the formate pathway follows reactions R1-R5, while the formation of CO through the RWGS pathway follows reactions R1-R2 and R6-R10. The optimized geometries for important adsorbates are presented in Figure 2. We will compare the turnover frequencies (TOFs) for these two reaction pathways on the Pd_7 and Pd_6M clusters to understand the selectivity of the clusters toward HCOOH production.

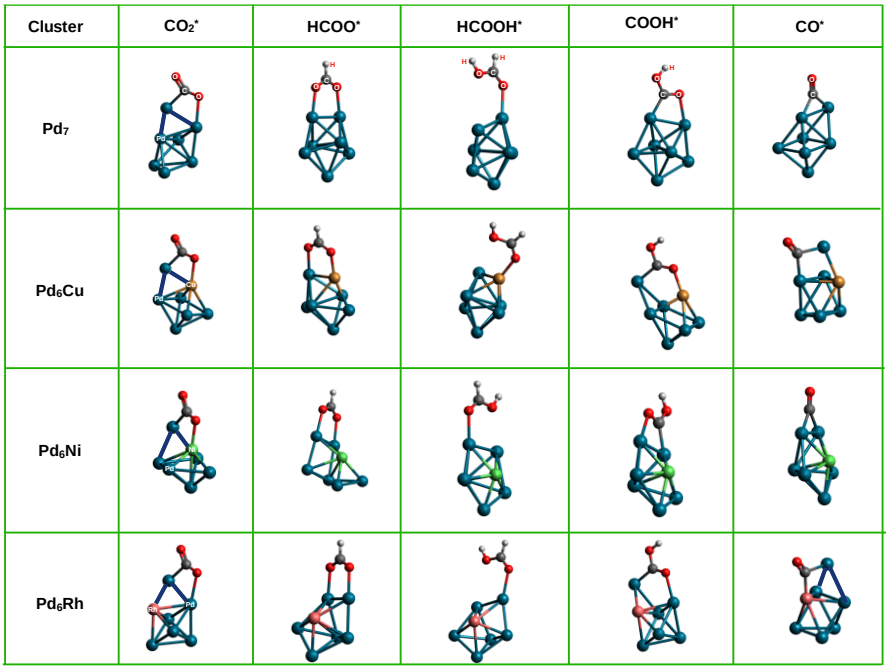

Figure 2 Optimized geometries for CO_2, HCOO, HCOOH, COOH, and CO adsorptions on the Pd_7 and Pd_6M clusters.

Table 1 Activation energies (E_{act}) and reaction energies (ΔE) for elementary reactions involved in the CO_2 hydrogenation to HCOOH and CO. All values are in eV.* and *X corresponds to the free adsorption site and adsorbed X species.

	Elementary Reaction	Pd_7 [13]		Pd_6Cu		Pd_6Ni		Pd_6Rh	
		E_{act}	ΔE	E_{act}	ΔE	E_{act}	ΔE	ΔE	E_{act}
R1	$H_{2(g)} + {}^* + {}^* \rightarrow H^* + H^*$	-	-0.73	-	-0.64	-	-0.58	-	-0.73
R2	$CO_{2(g)} + {}^* \rightarrow CO_2^*$	-	-0.21	-	-0.45		-0.40	-	-0.24
R3	$CO_2^* + H^* \rightarrow HCOO^* + {}^*$	0.93	-0.21	1.06	-0.31	0.87	-0.22	0.94	-0.19
R4	$HCOO^* + H^* \rightarrow HCOOH^* + {}^*$	1.16	0.94	1.05	1.05	1.05	0.72	1.19	1.02
R5	$HCOOH^* \rightarrow HCOOH_{(l)} + {}^*$		0.50		0.55		0.43		0.31
R6	$CO_2^* + H^* \rightarrow HOCO^* + {}^*$	1.90	0.39	1.92	0.48	0.80	0.27	1.71	0.22
R7	$HOCO^* + {}^* \rightarrow CO^* + OH^*$	0.44	-1.05	0.83	-0.88	1.04	-0.85	0.63	-0.51
R8	$CO^* + OH^* + H^* \rightarrow CO^* + H_2O^* + {}^*$	1.26	-0.17	1.12	-0.22	0.71	-0.47	0.84	-0.28
R9	$CO^* + H_2O^* \rightarrow CO^* + H_2O_{(l)} + {}^*$	-	0.51	-	1.16	-	0.44	-	0.35
R10	$CO^* \rightarrow CO_{(g)} + {}^*$	-	1.88	-	1.24	-	1.86	-	1.28

The energetical data in Table 1 were used as inputs for the microkinetic simulation to calculate the TOFs of the formate and RWGS pathways on the Pd_7 and Pd_6M clusters. The microkinetic simulation was done at p = 50 bar with CO_2:H_2 ratio of 1:1. These parameters were used to mimic the reaction conditions of direct CO_2 hydrogenation to HCOOH on supported Pd-Ni alloy nanoparticles on CNT-graphene in the absence of base additives [12]. A comparison of the TOFs of the formate and RWGS pathways is presented in Figure 3. It can clearly

be seen that the TOFs of HCOOH formation from the formate pathway were significantly larger than the TOFs of CO formation through the RWGS pathway. One of the reasons is that the activation energies for HOCO formation are in general larger than those for the HCOO formation. Moreover, the reaction profiles for HCOO formation are in general exothermic while the reaction profiles for HOCO formation are endothermic. These two factors make the initial step of CO_2 hydrogenation energetically prefer HCOO formation. The other reason is due to the strong CO adsorption energy on the Pd_7 and Pd_6M clusters (E_{ads}^{CO} is equivalent to the $-\Delta E$ value for reaction R10). The CO adsorption energies are significantly larger than the HCOOH adsorption energies (E_{ads}^{HCOOH} is equivalent to the $-\Delta E$ value for reaction R5). The very strong CO adsorption energy prevents the molecule to be desorbed as a product and this makes the TOF of CO production on Pd7 and Pd6M clusters become significantly lower than that of HCOOH production. The strongly adsorbed CO molecule may be reduced to HCO with high activation energy (E_{act} >1.4 eV [13]) or it may be reverted to CO_2 through the water-gas shift reaction. This result suggests that CO_2 hydrogenation on Pd_7 and Pd_6M clusters is indeed more selective towards HCOOH production than CO production.

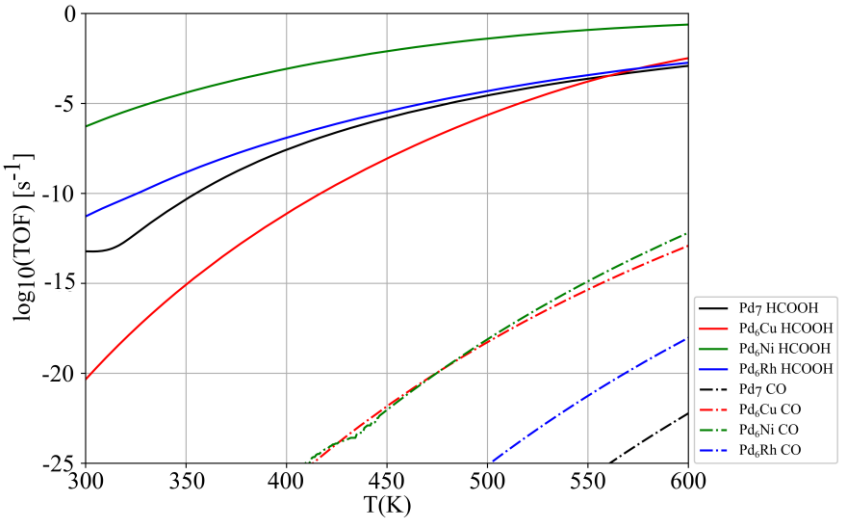

Figure 3 Comparison of TOFs for the formation of HCOOH and CO on the Pd_6M clusters at p = 50 bar and a CO_2:H_2 ratio of 1:1.

In general, the trend of the TOF for HCOOH formation on the Pd_6M system is the following: Pd_6Ni > Pd_6Rh > Pd_7 > Pd_6Cu. This trend shows that the inclusion of transition metal doping to the subnanometer Pd_7 cluster can really enhance the TOF for CO_2 hydrogenation to HCOOH, especially for Ni doping and Rh doping.

The trend of TOF towards CO_2 hydrogenation to HCOOH for Pd_6M clusters is explained as follows. The rate-limiting reaction for HCOOH formation on Pd_7 and Pd_6M clusters can be identified by analyzing the profile of the degree of rate control (XRC) as a function of temperature. An XRC_i of zero indicates that the rate constant of elementary step i has no effect on the overall rate constant, where $XRC_i = 1$ implies that step i determines the overall reaction rate [19,20]. The XRC for the Pd_7 system is presented in Figure 4 as an example,.

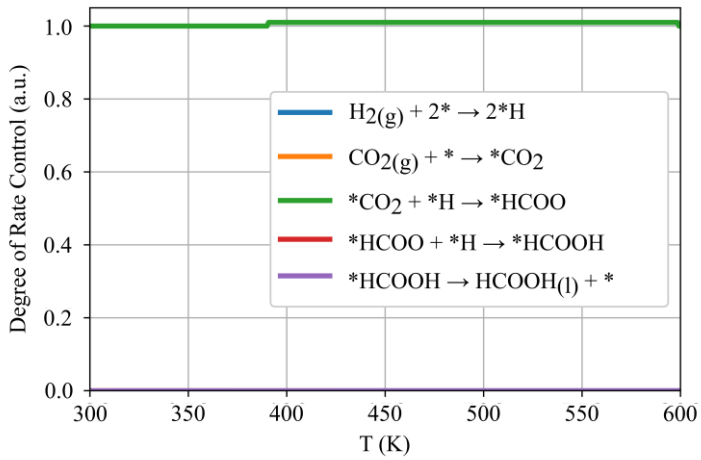

Figure 4 Degree of rate control (XRC) for CO_2 hydrogenation to HCOOH on the Pd_7 and Pd_6M clusters.

We find that the XRC for HCOOH formation on Pd_6M clusters actually has a similar profile as on the Pd_7 cluster. This means that the rate-limiting reaction for HCOOH formation on all of these clusters originates from the initial CO_2 hydrogenation step to formate (R3: CO_2* + H* → HCOO*), since this reaction dominates the XRC profile. Because all of the Pd_6M clusters exhibit similar XRC profiles, we can explain the trend of TOFs towards CO_2 hydrogenation to HCOOH by using the trend of activation energy (E_{act}) towards formate formation (R3). The trend of E_{act} versus TOF at the selected temperatures is given in Figure 5. We can see in general that the TOF increased as the E_{act} decreases. The Pd_6Ni cluster had the highest TOF because this system had the lowest activation energy for the initial CO_2 hydrogenation to formate.

The formation of formate requires two steps: (1) the bending of the linear O-C-O configuration, and (2) the desorption of an adsorbed H from the catalyst to the adsorbed CO_2 molecule [13,18,21]. The first condition is already fulfilled on Pd_7 and Pd_6M clusters due to the formation of CO_2 bidentate configuration. The second condition depends on the hydrogen adsorption energy on the cluster. The

Pd_6Ni cluster has the lowest activation energy for formate formation because this system has the weakest H adsorption energy, as indicated by the value of ΔE for R1 in Table 1. Interestingly, the inclusion of Ni doping to the Pd_7 cluster not only reduces the activation energy for formate formation, but also for the subsequent hydrogenation reaction (R4: HCOO* + H*→ HCOOH*) relative to the non-doped Pd_7 cluster system. These two conditions only occur in the Pd_6Ni system. This makes the Pd_6Ni system have the highest activity towards HCOOH production.

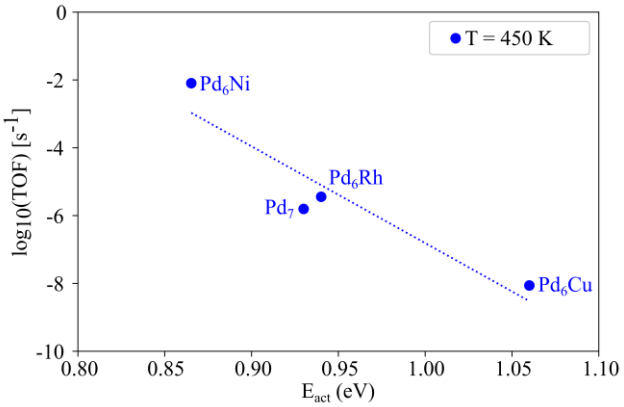

Figure 5 Comparison of activation energy (E_{act}) of formate formation (R3) versus TOF of CO_2 hydrogenation to HCOOH on the Pd_7 and Pd_6M clusters.

3.2 Trend of HCOOH Formation

In this subsection, we compare the TOF for CO_2 hydrogenation to HCOOH on the Pd_7 and Pd_6M clusters with other catalyst models. We used the energetical data available from the literature for HCOOH formation or decomposition as the inputs for microkinetic simulations to calculate the TOFs for CO_2 hydrogenation to HCOOH formation in the absence of base additives. We used the energetical data of a large Pd_{55} cluster [22] to represent the model of Pd nanoparticles. We also use the energetical data of flat Pd(111) [23], Cu(111) [24], Ni(111) [18,25,26], and Rh(111) [26,27] surfaces to show the initial activities of the transition metal M doping. The calculated TOFs are presented in Figure 6. The comparison was done at p = 50 bar with CO_2:H_2 ratio of 1:1.

In general, the TOF profiles for HCOOH reaction on Pd_6M clusters were relatively better than those on their respective M(111) surfaces, except for the Pd and Cu cases. In the Pd case, the TOFs of the pure Pd_7 cluster and Pd(111) surface were slightly smaller than that of the Pd_{55} cluster at low temperature region. However, their TOFs converged into the same value in a higher temperature

region. This suggests that Pd nanoparticles in pure form are more appropriate for low-temperature direct CO_2 hydrogenation to HCOOH catalyst than the subnanometer Pd_7 cluster and the Pd(111) surface. For the Cu case, the TOF of the Cu(111) surface in the low temperature region was much higher than that of the Pd_6Cu cluster. Interestingly, the Cu(111) surface also had the best TOF profile for HCOOH formation compared to the other flat metal surfaces in the low temperature region. The good TOF profile of the Cu(111) surface was in agreement with a recent experimental finding that showed the exceptional performance of Cu-based active sites in catalyzing CO_2 hydrogenation to HCOOH [28].

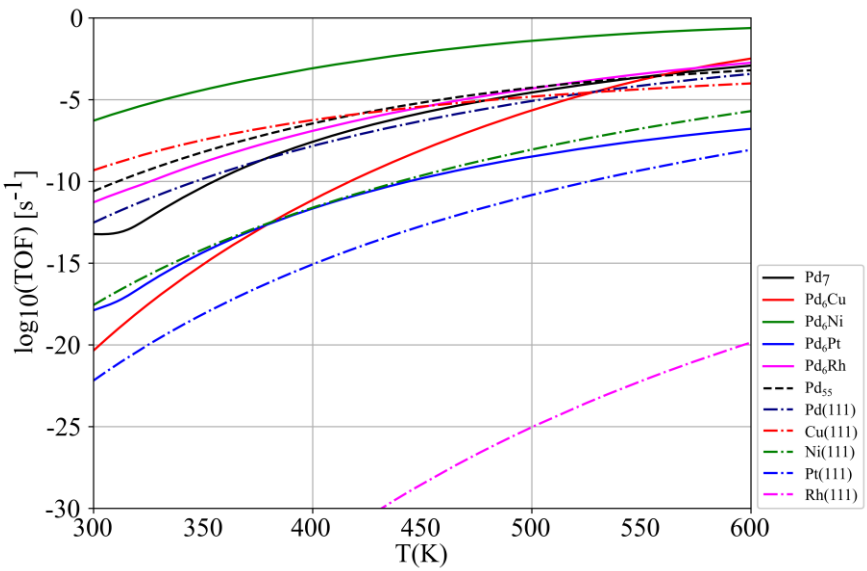

Figure 6 Comparison of turn-over frequencies (TOF) of CO_2 hydrogenation to HCOOH at p = 50 bar and CO_2:H_2 ratio of 1:1 for the Pd_7 and P_6M clusters with some metal surfaces.

The best TOF profile for HCOOH formation in this comparison was achieved in the Pd_6Ni cluster system. This system has superior TOF profiles in low and high temperature regions. This result suggests that the subnanometer Pd_xNi cluster may be used as a promising catalyst candidate for direct CO_2 hydrogenation to HCOOH. The activity of this catalyst can still be improved by optimizing several physical parameters. Our previous study showed that the size of the subnanometer Pd_x cluster affects the TOF for CO_2 hydrogenation to methanol [13]. The TOF increases as the size increases. However, at some point, the activity of the Pd cluster will decrease because a large size Pd island can only act as an H_2 dissociation center and not as a CO_2 hydrogenation center. Therefore, the activity of the Pd_xNi cluster towards CO_2 hydrogenation to HCOOH may be enhanced by

optimizing the cluster size. The alloy composition [12] and the type of support materials [11] are known to affect the catalytic activity of Pd nanoparticles. These two factors can also be optimized to improve the activity of the Pd_xNi cluster. These optimizations will be the main focus of our next works.

4 Conclusion

We studied direct CO_2 hydrogenation to HCOOH without the presence of base additives on the subnanometer Pd_7 cluster doped by transition metals (Pd_6M: M = Cu, Ni, Rh) by combining density functional theory calculations and microkinetic simulations. It was shown that the CO_2 hydrogenation on the Pd_7 and Pd_6M clusters are kinetically much more selective towards the formate pathway to produce HCOOH than the RWGS pathway to produce CO. We further found that inclusion of Ni and Rh doping to the subnanometer Pd_7 cluster could enhance the turnover frequency for CO_2 hydrogenation to HCOOH at low temperature. The order of TOF for HCOOH formation can be explained by the trend of the activation energy for the reaction $CO_2^* + H^* \rightarrow HCOO^*$. The Pd_6Ni cluster has the highest TOF because this cluster has the lowest activation energy for this formation. The Pd_6Ni system also has a superior TOF profile for HCOOH formation compared to several metal surfaces in low and high temperature regions. This finding suggests that the subnanometer Pd_xNi cluster is a promising catalyst candidate for direct CO_2 hydrogenation to HCOOH. The catalytic activity of the Pd_xNi cluster may be further improved by optimizing several parameters such as cluster size, Pd-Ni composition, and support material.

Acknowledgements

This work was funded by Institut Teknologi Bandung through the P3MI 2020 program. Some of the calculations were performed using the high-performance computing facilities at the Research Center for Nanosciences and Nanotechnology, Institut Teknologi Bandung.

References

[1] Abanades, J.C. Rubin, E.S. Mazzotti, M. & Herzog, H.J., *On the Climate Change Mitigation Potential of CO_2 Conversion to Fuels*, Energy Environ. Sci., **10**, pp. 2491-2499, 2017.

[2] Kätelhön, A., Meys, R., Deutz, S., Suh, S. & Bardow, A., *Climate Change Mitigation Potential of Carbon Capture and Utilization in the Chemical Industry*, Proc. Natl. Acad. Sci. U.S.A. 166, pp. 11187-11194, 2019.

[3] Mustafa, A., Lougou, B.G., Shuai, Y., Wang, Z. & Tan, H., *Current Technology Development for CO_2 Utilization Into Solar Fuels and Chemicals: A Review*, J. Energy Chem. **49**, pp. 96-123, 2020.

[4] Álvarez, A., Bansode, A., Urakawa, A., Bavykina, A.V., Wezendonk, T.A., Makkee, M., Gascon, J. & Kapteijn, F., *Challenges in the Greener Production of Formates/Formic Acid, Methanol, and DME by Heterogeneously Catalyzed CO_2 Hydrogenation Processes*, Chem. Rev. **117**, pp. 9804-9838, 2017.

[5] Behr, A. & Nowakowski, K., *Catalytic Hydrogenation of Carbon Dioxide to Formic Acid*, 1st ed.; Elsevier Inc., 66, 2014.

[6] Su, J., Yang, L., Lu, M. & Lin, H., *Highly Efficient Hydrogen Storage System Based on Ammonium Bicarbonate/Formate Redox Equilibrium Over Palladium Nanocatalysts*, ChemSusChem, **8**, pp. 813-816, 2015.

[7] Bi, Q.Y., Lin, J.D., Liu, Y.M., Du, X.L., Wang, J.Q., He, H.Y. & Cao, Y., *An Aqueous Rechargeable Formate-based Hydrogen Battery Driven by Heterogeneous Pd Catalysis*, Angew. Chemie – Int. Ed. **53**, pp. 13583-13587, 2014.

[8] Mori, K., Sano, T., Kobayashi, H. & Yamashita, H., *Surface Engineering of a Supported PdAg Catalyst for Hydrogenation of CO_2 to Formic Acid: Elucidating the Active Pd Atoms in Alloy Nanoparticles*, J. Am. Chem. Soc., **140**, pp. 8902-8909, 2018.

[9] Lee, J.H., Ryu, J., Kim, J.Y., Nam, S.W., Han, J.H., Lim, T.H., Gautam, S., Chae, K.H. & Yoon, C.W., *Carbon Dioxide Mediated, Reversible Chemical Hydrogen Storage Using a Pd Nanocatalyst Supported on Mesoporous Graphitic Carbon Nitride*, J. Mater. Chem., **A2**, pp. 9490-9495, 2014.

[10] Wang, F., Xu, J., Shao, X., Su, X., Huang, Y. & Zhang, T., *Palladium on Nitrogen-doped Mesoporous Carbon: A Bifunctional Catalyst for Formate-based, Carbon-neutral Hydrogen Storage*, ChemSusChem, **9**, pp. 246-251, 2016.

[11] Zhang, Z., Zhang, L., Yao, S., Song, X., Huang, W., Hülsey, M.J. & Yan, N., *Support-dependent Rate-determining Step of CO2 Hydrogenation to Formic Acid on Metal Oxide Supported Pd Catalysts*, J. Catal., **376**, pp. 57-67, 2019.

[12] Nguyen, L.T.M., Park, H., Banu, M., Kim, J.Y., Youn, D.H., Magesh, G., Kim, W.Y. & Lee, J.S., *Catalytic CO_2 Hydrogenation to formic Acid Over Carbon Nanotube-graphene Supported PdNi Alloy Catalysts*, RSC Adv., **5**, pp. 105560-105566, 2015.

[13] Saputro, A.G., Putra, R.I.D., Maulana, A.L., Karami, M.U., Pradana, M.R., Agusta, M.K., Dipojono, H.K. & Kasai, H., *Theoretical Study of CO_2 Hydrogenation to Methanol on Isolated Small Pdx Clusters*, J. Energy Chem., **35**, pp. 79-87, 2019.

[14] Saputro, A.G., Agusta, M.K., Wungu, T.D.K., Suprijadi, Rusydi, F. & Dipojono, H.K., *DFT Study of Adsorption of CO_2 on Palladium Cluster Doped by Transition Metal*, Journal of Physics: Conference Series, **739**(1), 012083, 2016.

[15] Li, S.J., Zhou, X. & Tian, W.Q., *Theoretical Investigations on Decomposition of HCOOH Catalyzed by Pd 7 Cluster*, J. Phys. Chem. A **116**, pp. 11745-11752, 2012.
[16] Saputro, A.G., Fajrial, A.K., Maulana, A.L., Fathurrahman, F., Agusta, M.K., Akbar, F.T. & Dipojono, H.K., *Dissociative Oxygen Reduction Reaction Mechanism on the Neighboring Active Sites of Boron-doped Pyrolyzed Fe-N-C Catalyst*, J. Phys. Chem., **C 124**(21), pp. 11383-11391, 2020.
[17] Saputro, A.G., Akbar, F.T., Setyagar, N.P.P., Agusta, M.K., Pramudya, A.D. & Dipojono, H.K., *Effect of Surface Defects on the Interaction of the Oxygen Molecule with the ZnO(10$\bar{1}$0) Surface*, New J. Chem., **44**, pp. 7376-7385, 2020.
[18] Maulana, A.L., Putra, R.I.D., Saputro, A.G., Agusta, M.K., Nugraha, N. & Dipojono, H.K., *DFT and Microkinetic Investigation of Methanol Synthesis via CO_2 Hydrogenation on Ni(111)-based Surfaces*, Phys. Chem. Chem. Phys., **21**, pp. 20276-20286, 2019.
[19] Campbell, C.T., *Future Directions and Industrial Perspectives Micro- and Macro-kinetics: Their Relationship in Heterogeneous Catalysis*, Top. Catal., **1**, pp. 353-366, 1994.
[20] Stegelmann, C., Andreasen, A. & Campbell, C.T., *Degree of Rate Control: How Much the Energies of Intermediates and Transition States Control Rates*, J. Am. Chem. Soc., **131**, pp. 13563, 2009.
[21] Nugraha Saputro, A.G. Agusta, M. K. Rusydi, F. Maezono, R. & Dipojono, H.K., *DFT Study of the Formate Formation on Ni(111) Surface Doped by Transition Metals [Ni(111)-M; M=Cu, Pd, Pt, Rh]*, Journal of Physics: Conference Series, **739**, 012082, 2016.
[22] Liu, D., Gao, Z.Y., Wang, X.C., Zeng, J. & Li, Y.M., *DFT study of Hydrogen Production from Formic Acid Decomposition on Pd-Au Alloy Nanoclusters*, Appl. Surf. Sci., **426**, pp. 194-205, 2017.
[23] Zhang, M., Wu, Y., Dou, M. & Yu, Y., *A DFT Study of Methanol Synthesis from CO2 Hydrogenation on the Pd(111) Surface*, Catal. Letters **148**, pp. 2935-2944, 2018.
[24] Grabow, L.C. & Mavrikakis, M., *Mechanism of Methanol Synthesis on Cu through CO2 and CO Hydrogenation*, ACS Catal., **1**(4), pp. 365-384, 2011.
[25] Peng, G., Sibener, S. J., Schatz, G.C., Ceyer, S. T. & Mavrikakis, M., *CO_2 Hydrogenation to Formic Acid on Ni(111)*, The Journal of Physical Chemistry C, **116**(4), pp. 3001-3006, 2012.
[26] Herron, J.A., Scaranto, J., Ferrin, P., Li, S. & Mavrikakis, M., *Trends in Formic Acid Decomposition on Model Transition Metal Surfaces: A Density Functional Theory Study*, ACS Catal., **4**, pp. 4434-4445, 2014.
[27] Hu, C., Ting, S.W., Chan, K.Y. & Huang, W., *Reaction Pathways Derived from DFT for Understanding Catalytic Decomposition of Formic Acid Into*

Hydrogen on Noble Metals, Int. J. Hydrogen Energy **37**, pp. 15956-15965, 2012.

[28] Chiang, C.L., Lin, K.S. & Chuang, H.W., *Direct Synthesis of Formic Acid Via CO2 Hydrogenation Over Cu/ZnO/Al2O3 Catalyst*, J. Clean. Prod., **172**, pp. 1957-1977, 2018.